High Frequency Membrane Hydrophone

P. Lum and M. Greenstein
Hewlett-Packard Laboratories, Palo Alto, CA 94303
C. Grossman and T. L. Szabo
Imaging Systems Division, Hewlett-Packard, Andover, MA 01810

Abstract

A membrane hydrophone with a 37 μm diameter spot poled electrode has been fabricated on a 4 μm thick film of the piezoelectric copolymer, Polyvinylidene fluoride trifluoroethylene (PVDF-TrFE), and initially characterized. The hydrophone has an effective spot size of less than 100 μm, an on-membrane +7 dB gain buffer amplifier, and a -3 dB bandwidth of 150 MHz. The acoustic properties of the hydrophone were investigated with a transducer equivalent circuit model, the electric fringe fields due to poling were characterized with a finite difference electrostatic field model, and the effective spot diameters $2a_3$ and $2a_6$ were estimated. Measurements on the bandwidth, effective spot size, and sensitivity are presented. This hydrophone appears suitable for the characterization of both the frequency and spatial parameters of high frequency transducers such as intravascular ultrasound (IVUS) catheter transducers operating in the 10 - 40 MHz range.

I. Introduction

The characterization of the ultrasonic acoustic field generated by ultrasonic medical instrumentation requires both spatial and temporal measurements. Specifications for the measurement of the temporal and spatial distribution of the radiated ultrasonic energy resulting from medical ultrasound transducers are well documented in the NEMA [1] and the IEC [2] voluntary standards. General coverage of this topic of ultrasonic exposimetry has been presented by Ziskin and Lewin [3].

Internal Accession Date Only

The typical hydrophones used in the medical imaging industry, with a -3 dB bandwidth of up to 20 MHz, and a geometric spot size of 500 μm [4], are appropriate tools to characterize acoustic imaging transducers in the frequency range of 1 to about 5 MHz. Recent advances have produced a 50 MHz hydrophone with a 200 μm geometric spot size [5]. Smith [6] discussed the need for higher bandwidth hydrophones to measure the center frequency of a transducer, and the higher harmonics generated through nonlinear propagation effects in water. There are new ultrasonic imaging modalities such as Intravascular Ultrasound (IVUS) in the 10 to 30 MHz frequency region which can not be adequately characterized by 15 to 20 MHz bandwidth hydrophones. Peak pulse parameters calculated from data measured with hydrophones with inadequate frequency response show large errors.

Smith [7], also addressed the issues of the hydrophone effective spot diameter. Effective spot sizes that are too large cause an averaging of the acoustic pressure over the active element which and an underestimation of the spatial-peak acoustic pressure. In the past, a correction factor has been used to compensate for these errors, however, disagreements between the theoretical and experimental corrected measurements were found. Smith concludes that in order to avoid corrections of up to 20% on peak pressures and 40% on peak intensities, hydrophones with adequate effective spot sizes are necessary.

The NEMA [1] and IEC [2] standards specify the effective spot diameter, D_e, for a hydrophone as a function of the wavelength, λ, the source diameter, d_s, and the hydrophone-to-transducer range, z, as

$$D_e \leq \frac{\lambda z}{2 d_s}. \tag{1}$$

In Fig. 1, D_e is plotted as a function of the source transducer frequency, $f = c/\lambda$, for various ratios of z/d_s. From Eq. (1), it can be seen that for a 30 MHz transducer, with a typical 1 mm

aperture, a transducer-to-hydrophone range of < 2 mm, and a ratio of $z/d_s \leq 2$, the required effective spot diameter is on the order of 50 μm.

Thus, there is an important need for hydrophones capable of characterizing transducers with frequency components in the range of 100 MHz and spatial resolution of typically less than 50 μm. This paper describes the modelling, fabrication and initial characterization of a membrane hydrophone fabricated from a 4 μm thick film of spot poled Polyvinylidene fluoride trifluoroethylene (PVDF-TrFE), with on-membrane electronics, a -3 dB bandwidth in excess of 150 MHz and a measured effective spot diameter of less than 100 μm.

II. Modelling Results

A. Acoustic Modelling

As a guide to fabrication, an acoustic modelling program [8], which implements the KLM model, was used to simulate the membrane hydrophone, including the effect of spot size, film thickness, electrical impedance loading from 50 Ω cables, and mass loading from electrodes. The material properties used in the model are taken from Toray [9], and can be found in Ohigashi and Koga [10]. The major differences in the material properties between the copolymer PVDF- TrFE used here, and the more commonly used PVDF, are the 1.4x increase in dielectric constant, the 1.9x increase in effective coupling coefficient, and the 0.63x decrease in the electrical loss tangent of the copolymer, PVDF-TrFE.

The effect of spot size is seen in the electrical impedance, $Z = \frac{1}{j2\pi f C_0} = \frac{t}{j2\pi f \varepsilon_0 A}$, where t is the thickness, A is the area of the geometric spot, and ε_0 is the clamped dielectric constant. Z varies inversely with the square of the geometric spot diameter and linearly with the membrane thickness. For a 4 μm thick membrane with 37 μm diameter geometric spot, this impedance approaches 10^5 Ω.

The structural thickness mode resonance frequency, f_0, of the membrane is given approximately by $f_o = c/(2t)$, where c is the velocity and t is the thickness of the membrane. It is important to have the thickness resonance beyond the measurement frequency of interest in order to maximize the flatness of the sensitivity. For a desired bandwidth in excess of 150 MHz, a 4 μm film is required. As the film thickness decreases, the sensitivity drops because the sensitivity is proportional to the thickness. In Fig. 2a the unloaded open circuit sensitivity, M_{oc}, is plotted against frequency for membrane thicknesses of 4, 9, 25, and 50 μm with a constant geometric spot diameter of 500 μm. This gives a relative comparison of the frequency response, and sensitivity. With decreasing thickness, the thickness resonance moves up in frequency and the peak sensitivity drops.

At these frequencies, the thickness resonance is affected by the mass of the deposited metal electrodes. For the 4 μm thick films used here, conventional 3000 A metal electrodes substantially degrade the peak frequency of the sensitivity, and the fractional bandwidth of the hydrophone response. A choice of 1000 A electrodes is a compromise between the need for a corrosion resistant electrode with adequate sheet resistance and the degradation of the bandwidth parameters.

For typical bilaminar hydrophones of 50 μm thickness, a 1 m coaxial cable is often used to tune the electrical impedance of the hydrophone circuit. In Fig. 2b, the effect of various lengths of 50 Ω cable from 1 m to 0.10 m are shown on a 4 μm thick film with a 500 μm geometric spot diameter. The 1 m cable now introduces an unacceptable resonance at ~ 110 MHz. At a cable length of 0.25 m, the resonant frequency properties are recovered, but with a -58 dB loss in sensitivity. A 4 μm thick, 150 MHz bandwidth hydrophone thus requires on-membrane electronics to avoid corrupting the frequency characteristics, or introducing unacceptable loss in sensitivity.

B. Electrostatic Fringe Field Modelling

Although the geometrical size of the spot electrode is 37 μm, during the spot poling process the high electric fields have fringe fields that extend beyond the edge of the spot electrode, and increase the effective spot size. These fringe fields may pole areas of the piezoelectric polymer beyond the intended spot electrode. In order to estimate the magnitude of the fringe fields, an electrostatic field modelling program [11] was used to model the electrical field patterns. Voltages on the structure are specified, and Poisson's equation is solved iteratively, in 3 dimensions. The geometry of the model is shown in Fig. 3a, a 37 μm diameter spot electrode with a 37 μm wide trace on a 4 μm thick film. The underlying ground plane overlaps the spot electrode completely. In Fig. 3b contour plots of the electrical potential at 5% incremental values are shown for a cross section at x=50 μm. On each side of the structure, out to an additional ~5 μm, the potential is still greater than 50% of the maximum potential on the electrode. This predicts a total effective "poled" spot diameter of ~10 μm greater than the geometric electrode, or ~ 47 μm. Equivalent results are seen in the orthogonal cross section.

C. Directivity Modelling

For an ideal circularly symmetric uniform ultrasound transducer of radius b, its transmitted beam pattern near the beam axis either for the far field (if the transducer is unfocused) or for the geometric focus (if it is focused), is

$$T(\theta, z) = \left(\frac{j\pi b^2}{\lambda z}\right) \times \frac{2J_1((2\pi b \sin\theta)/\lambda)}{(2\pi b \sin\theta)/\lambda} \tag{2}$$

$$T(r, z) \approx \left(\frac{j\pi b^2}{\lambda z}\right) \times \frac{2J_1((2\pi b r)/(z\lambda))}{(2\pi b r)/(z\lambda)} \tag{3}$$

where J_1 is the Bessel function of the first kind, λ is the acoustic wavelength in water, r is the radial distance, z is the axial distance from the transducer, and $\theta = \arctan r/z$. Note that if the transducer is focussed, $z = f$, the geometric focal length. On reception, similar arguments provide the directivity of an ideal stiff disc hydrophone of radius a,

$$D(\theta, z) = \left(\frac{j\pi a^2}{\pi z}\right) \times \frac{2J_1((2\pi a \sin\theta)/\lambda)}{(2\pi a \sin\theta)/\lambda} \tag{4}$$

In reality, the construction of a practical hydrophone may cause its actual directivity to deviate from this ideal.

If an ideal beam of the type described by Eq. (2) and Eq. (3) were incident on a hydrophone, the measured field can be modelled to a good approximation as the spatial average over the hydrophone area. Along a radial dimension, the measured field is the running mean of the transmitted field from Eq. (3),

$$R(r, z) = \frac{1}{a} \times \int_{r-\frac{a}{2}}^{r+\frac{a}{2}} T(r', z)\, dr' . \tag{5}$$

Thus, Eq. (5) can be used to predict the measured hydrophone response.

III. Fabrication Process

A. Materials

This section describes the fabrication process for the hydrophone beginning with a brief description of the physical material properties of the polymers and copolymers. The subsequent sections describe the patterning to define the electrodes on the films, the poling to create the active area, the on-membrane electronics, and finally the fabrication process flow.

The piezoelectric polymers usually have a higher maximum frequency response than the ceramics, and are thus generally preferred for high frequency applications. A summary of the relevant PVDF and PVDF-TrFE properties can be found in Ohigashi & Koga [10]. The superior coupling of PVDF-TrFE, as compared to PVDF, was one of the reasons it was selected as

the material of choice. Lovinger [12], Ohigashi & Koga [10], and Brown [13] discuss further details of the polymers and copolymers.

B. Patterning

The patterning of the piezoelectric film to obtain an appropriately small diameter spot electrode can be achieved by several process techniques. One process involves photolithography techniques that have been used in integrated circuit processing and surface acoustic wave devices [14], [15], [16]. A second method of patterning the metal deposited on the membrane film involves shadow-masking [17]. In this procedure a thin metal pattern covers all but the locations to receive the electrode pattern. The metal is then deposited through holes in the mask. The copolymer, PVDF-TrFE, is degraded by several common solvents used in photolithography. For this reason, an electroformed nickel shadow mask [18] was selected to define the hydrophone metal pattern structures.

C. Poling

The crystalline structure and phase transition of the copolymers depends upon the vinylidene fluoride content. When the film material is mechanically deformed or electrically poled, its domains are transformed to regular all-trans chains [19]. Raw piezoelectric PVDF or PVDF-TrFE film as received from a vendor [20] is generally unpoled with unaligned ferroelectric domains. The poling procedure for PVDF requires a combination of mechanical deformation, temperature and electrical field [22] and [23]. The procedure for PVDF-TrFE requires only temperature and an electrical field. The PVDF-TrFE was poled at 130 degrees Centigrade at 70 V/μm in vacuum. The temperature also serves to anneal the film [22] and [23].

D. Electrical Properties

As discussed in Section IIA, the expected bandwidth of a 4 μm thick hydrophone extends up to nearly 200 MHz, and the electrical impedance increases above 10^5 Ω. It is desired that over

this frequency range the sensitivity be moderately flat. When this flatness in the sensitivity from 1 MHz to 200 MHz is combined with the need to match the electrical impedance of 10^5 Ω, a very wide bandwidth buffer amplifier, placed very close to the hydrophone spot electrode, with a high input impedance is needed. An AD9630 buffer amplifier with low distortion, 450 KΩ input impedance, and a 750 MHz bandwidth was selected [24]. This amplifier has a frequency response of +/- 1 dB out to 300 MHz. The amplifier is surface mounted onto the membrane at a distance of 10 mm, sufficient as to not distort the acoustic waveform arriving from a typical IVUS transducer of less than 1 mm diameter.

E. Construction

The fabrication of a membrane hydrophone begins with the raw film, in a roll form, supplied by a vendor [20]. The front side is first patterned for the active spot electrode and all associated on-membrane electronics connections. The backside is then patterned for the ground plane. Alignment of the ground plane relative to the spot electrode is necessary to correctly establish the overlap of the spot electrode. The membrane is then mounted onto the hydrophone hoop.

Poling is then performed, and an additional metal ground plane is deposited on the backside of the hydrophone. Surface mount components and connectors are directly mounted onto the membrane surface with conductive epoxy. A Silicone elastomer, Silgard 186 [21] with an acoustic impedance of 1.15, is cast over the entire backside of the membrane to encapsulated the electronics and provide a structural backing.

A photograph of the rear surface of the hydrophone is shown in Fig. 4a. Here the support ring can be seen. The ground plane is on the left side of the membrane. The spot electrode is at the end of the trace pointing toward the center of the membrane. The on-membrane electronics are located in the upper right portion of the photo, with two power supply leads shown on the

left side of the photo. The hydrophone is terminated into a standard BNC type 50 Ω connector. The additional post-poling ground plane mentioned above is not shown in this photograph, since it would obscure all of the front side patterns from view. In Fig. 4b a photomicrograph of the active area is shown. Here the top surface electrode is seen as it tapers down to the 37 μm diameter active spot electrode. The ground plane is located in the top half of the picture, under the piezoelectric film, where it just overlaps the 37 μm active spot electrode.

IV. Experimental Methods and Results

A. Bandwidth

One of the key design parameters for the hydrophone is the desired frequency response, a bandwidth of at least 150 MHz. Several potential methods for measuring the bandwidth include calibration against known standard hydrophones, interferometry, reciprocity, and the shock wave method. Unfortunately, there are no widely accepted acoustic standard methods to calibrate hydrophones above about 20 MHz. At the present, the optical interferometric techniques used at the National Physical Laboratories [25] could be extended to 50 MHz, though it is not commercially available. As a result, Bacon's shock wave method [26] was chosen to evaluate the present hydrophone.

In the shock wave method, a source transducer is driven to produce nonlinear effects [27], [28], [29] in the water propagation medium. In a fully developed shock wave, a classic "N" wave may be formed. Nonlinearity of the speed of the acoustic signal in water causes a cumulative distortion of the propagating waveform. When the waveform distorts in time, new frequency components are generated and these frequency components are harmonically related. As a result, the frequency spectrum of an ideal N shaped shock wave is expected to have har-

monic frequency components at multiples of the fundamental, n=1, 2, 3, 4,... [30], each of which has an amplitude 1/n.

If the harmonic amplitude fall off and the attenuation of the water are known, then the absolute hydrophone response can be inferred from the hydrophone's response to an ideal "N" wave. The shock wave calibration method has been used successfully at the National Physical Laboratories under specified conditions [31]. Unfortunately, perfect "N" waves are rarely achieved in the fields of medical ultrasound transducers. Because of finite bandwidth limitations, attenuation effects are often not known precisely enough over the entire bandwidth, (here 300 MHz). Diffraction phase effects in the beam [32] prevent ideal "N" waveforms from being realized experimentally. Shock excitation, however, can provide an extremely broadband signal to aid in the evaluation of a hydrophone bandwidth.

The waveform shown in Fig. 5a depicts the shock waveform obtained from a 20 MHz 6.4 mm diameter focused transducer at a focal distance of 19 mm. The source transducer is pulsed with a high voltage. An imperfect N shaped waveform can be observed in the figure. The -3 dB bandwidth can be estimated from the compressional portion of this waveform. Depicted in the dotted ellipse is the 10% to 90% rise time of 2.3 ns. From this rise time a bandwidth of 150 MHz is calculated. The related frequency spectrum is shown in Fig. 5b. The harmonics can be seen from 1 (at 15.6 MHz) to 20 (at 315 MHz).

Waveform measurements were also made using a Hewlett Packard Sonos 2500 imaging system with a 5.5 MHz phased array transducer as a source. Two hydrophones were used to measure the acoustic waveform at focus. The first hydrophone was a calibrated Marconi [4] bilaminar hydrophone with a 500 μm geometric spot diameter on a 50 μm PVDF membrane and a 6 dB external amplifier at the end of the cable. The second hydrophone was the present hydrophone with a 37 μm geometric spot on a 4 μm thick membrane, a 7dB on-membrane amplifier and a 25 dB broadband amplifier at the other end of the cable. Fig. 6a shows the fre-

quency spectrum using the Marconi hydrophone. The inset shows the nonlinear measured waveform. The spectrum shows the fundamental at 5 MHz and three harmonics at 10, 15, and 20 MHz before the signal falls into the noise floor. Fig. 6b shows the frequency spectrum using the present hydrophone. The inset shows the respective waveform with greater detail due to the greater bandwidth. The spectrum shows the fundamental at 5 MHz and the subsequent 40 harmonics out to 200 MHz. This data correlates well with the bandwidth measurement estimates shown in Fig. 5a and b. Figure 6 also indicates comparable M_L sensitivities for both hydrophones at 5 MHz with this particular set of amplifiers.

B. Effective Spot Size

Both planar scanning and angular measurement techniques can be used to estimate the effective spot size of a hydrophone. In the planar scanning method, discussed by Herman and Harris [33], a hydrophone is scanned across the far field of an unfocused transducer to produce a beam profile. The effective spot size can then be inferred from the beam width profile providing the beam cross section is small relative to the hydrophone diameter at the specified wavelength. Evaluating geometric spot diameters on the order of 50 μm using this method is technically challenging. A reduction in transmitted beam size can be made by using a beam profile at the geometric focus of a transducer because the shape of the beam there is identical to that in the far field of an unfocused transducer, according to Eq. (2) and Eq. (3).

Results for two hydrophone measurements, one from a bilaminar 500 μm geometric spot diameter Marconi hydrophone and another from the 37 μm geometric spot diameter hydrophone are shown in Fig. 7. The ideal transmitted beam as calculated by Eq. (3) for a 20 MHz 6.35 mm diameter, 19.05 mm focal length source, is compared with simulations from Eq. (5) for a 500 μm diameter hydrophone, in Fig. 7a, and a 37 μm diameter hydrophone in Fig. 7b, each of which has been normalized to the corresponding data. The small differences in sidelobes

between the simulations and the data can be attributed to slight uncertainties in the location of the transducer focus. Note that the 37 μm hydrophone nearly duplicates the shape of the transmitted beam, whereas the 500 μm diameter hydrophone underestimates the amplitude by 40% and overestimates the -6 dB beamwidth of the transmitted beam by 50%. For this case in which the transmitted -3 dB beamwidth is on the order of 230 μm, simulations for receive diameters of 100 μm or less were found to give equivalent results. Therefore this data can only place a upper bound of 100 μm on the hydrophone effective spot size

In the angular response method, discussed by Shombert, Smith, and Harris [34], the directional response given by Eq. (4) can be measured and used to estimate the effective diameter. For a given frequency, f, the -3 and -6 dB points of the directional response correspond to particular half angle values of θ_3 and θ_6, respectively. The following equations, derived from Eq. (4), can then be used to relate the effective spot size diameters, $2a_{-3dB}$ and $2a_{-6dB}$ to their respective half angles [1]:

$$2a_{-3dB} = (1.62)\frac{c}{\pi f \sin\theta_3}, \tag{6}$$

$$2a_{-6dB} = (2.22)\frac{c}{\pi f \sin\theta_6}. \tag{7}$$

As in the planar scanning method, the same focused 20 MHz transmitter was used to reduce the measurement distance by an order of magnitude over that needed for an unfocused transducer of the same size and frequency. This shorter distance reduces the water path attenuation by about 10 dB at 20 MHz. The same Eq. (6) and Eq. (7) can be used as discussed in Section II.

When both equations are applied to the measured directional response in Fig. 8, the equations yield half angles corresponding to effective diameters of 104 to 100 μm. Lamb wave propagation appears at +/- 18 degrees on the directional response plots in the form of side lobes.

This behavior is unique to membrane hydrophones [26]. The size of the transmitted beam of the 20 MHz source transducer was the limiting factor in determining the resolution of a hydrophone at different angles. As in the planar scanning method, the angular response approach with this source indicates only an upper bound of 100 μm for the effective spot diameter. Further work is required to improve the measurement precision in order to resolve smaller spot sizes.

C. Sensitivity

Hydrophone sensitivity has been extensively discussed by Chivers and Lewin [35], [36] and by Harris [37]. The sensitivity of a membrane hydrophone is determined by the structural resonance of the membrane film, and the electrical and piezoelectric properties of the PVDF-TrFE material. For a hydrophone with a spot poled electrode area and an interconnecting lead attached to the electrode, the open circuit voltage sensitivity, M_{oc}, is given by the ratio of the developed voltage, V, and the incident acoustic pressure, P,

$$M_{oc} = \frac{V}{P} = (gtC_{sp}) / (C_{sp} + C_s), \tag{8}$$

where g is the voltage sensitivity, t is the thickness, and C_{sp} and C_s are the spot electrode capacitance and lead shunt capacitance, respectively. If the shunt capacitance of the lead, C_s, were to greatly exceed the capacitance of the poled spot electrode, C_s, the voltage sensitivity of the hydrophone will be dominated by the electrode and lead area. To avoid this problem, a buffer amplifier located as close as possible to the spot electrode is important. Earlier work by DeReggi [38], Harris [17] [39], Lewin [40], and Lum [41] have discussed the effect of a preamplifier with minimal lead length.

It is difficult to measure the open circuit sensitivity of the present hydrophone. Comparisons were made between the loaded end-of-cable sensitivity, M_L (Re 1 V/MPa), for a standard

Marconi hydrophone with an external amplifier of 6 dB, and the present hydrophone with an on-membrane amplifier of 7 dB and an external 25 dB amplifier. The results are presented in Table 1 for frequencies of 5, 10, 15 and 20 MHz. The measured loaded end-of-cable sensitivity, M_L (Re 1 V/MPa), of the present hydrophone, with amplifiers, was found to have a mean value of -2.5 dB less than the Marconi reference hydrophone for frequencies from 5 to 20 MHz, by this substitution method. The data from Table 1 can also be used to calibrate the vertical scales in the frequency plots of the shock wave measurements. In Fig. 5b the peak at 15.6 Mhz is at a value of M_L = -21 dB (Re 1V/MPa), and in Fig. 6, the peaks at 5 MHz are at a value of M_L = -25 dB (Re 1V/MPa).

The loaded end-of-cable sensitivity of the hydrophone was modelled[8] using a simple ideal transformer to represent the buffer amp. This model successfully predicted the relative flatness of the sensitivity data in the 5-20 MHz range, seen in Table 1, however this limited model did not accurately predict the absolute sensitivity level for the combination of the hydrophone, 7 dB on-membrane buffer amp, 50 Ω cable, and 25 dB external amplifier.

Although measurements are required out to 200 MHz to fully evaluate the present hydrophone's full range of sensitivity, there is not yet a satisfactory calibration procedure in this range. The best technique, known to the authors, is the reciprocity method which currently extends only to 50 MHz [42].

V. Summary

The result of this work is a membrane hydrophone fabricated on a 4 μm thick membrane film of PVDF-TrFE, a geometric spot diameter of 37 μm, a measured effective active spot less than 100 μm in diameter, with 1000 Angstrom thick electrodes, an on-membrane buffer amplifier within 10 mm of the active spot electrode, and a mean loaded end of cable sensitivity of -23 dB (Re 1V / MPa) in the range 5 to 20 MHz. The shock wave method was used to evaluate the

bandwidth. The substitutional method was used to evaluate the sensitivity up to 20 MHz. Directivity measurements with a 20 MHz focussed transducer established an upper limit for the effective spot diameter. Additional work is needed to determine the absolute hydrophone response in the range of 20 to 150 MHz, and to more accurately measure the effective spot size.

VI. Acknowledgements

The authors gratefully acknowledge Belinda Kendle for help with hydrophone fabrication, Ed Verdonk and Said Bolorforosh for many useful discussions, Henry Yoshida for the poling system, Jerry Zawadzki for numerous fixtures, and Pete Melton and Kate Stohlman for their continual support and encouragement.

VII. REFERENCES

[1] NEMA Standards Publication No. UD 2-1992, *Acoustic Output Measurement Standard For Diagnostic Ultrasound Equipment*. Published by National Electrical Manufacturers Association, 2101 L Street, N.W. Washington, D.C. 20037.

[2] IEC 1102:1991, *Measurement and Characterization of Ultrasonic Fields Using Hydrophones in The Frequency Range 0.5 MHz to 15 MHz*.

[3] M.C. Ziskin and P.A. Lewin, *Ultrasonic Exposimetry*, (1993), ISBN 0-8493-6436-1.

[4] GEC-Research Ltd., Marconi Research Center, Chelmsford, United Kingdom.

[5] Sonic Technology, 2935 Byberry Road, Hatboro, PA.

[6] R. A. Smith, *The Importance Of The Frequency Response Of A Hydrophone When Characterising Medical Ultrasonic Fields*, Proceedings Of The Institute Of Acoustics, Vol 8, Part2, 119-128, (1986).

[7] R. A. Smith, *Are Hydrophones Of Diameter 0.5 mm Small Enough To Characterise Diagnostic Ultrasound Equipment?*, Phys. Med. Biol., Vol 34, No 11, 1593-1607, (1989).

[8] "*PiezoCAD*" program from Sonic Concepts, Woodinville, WA.

[9] Toray Industries, Inc., 2,2 - Chome, Nihonbashi - Muromachi, Chuo-Ku, Tokyo, Japan.

[10] H. Ohigashi and K. Koga, *Ferroelectric Copolymers of Vinylidenefluoride and Trifluoroethylene with A Large Electromechanical Coupling Factor*, Japanese J of Applied Physics, Vol. 21, No. 8, (Aug 1982), L455-L457.

[11] "*Raphael*" program from Technology Modeling Associates, Palo Alto CA.

[12] A.J. Lovinger in D.C. Bassett, *Developments in Crystalline Polymers*, (Applied Science Publishers, London, 1981).

[13] L.F. Brown Dissertation entitled: *Electromechanical Modeling, Performance Testing. and Design of Piezoelectric Polymer Film Ultrasound Transducers* (1988).

[14] M. Hatzakis, B.J. Canavello, J.M. Shaw, *Single-Step Optical Lift-Off Process*, IBM J. Res. Develop, Vol 24, No 4, (July 1980).

[15] P.Lum, B.J. Kendle, M. Greenstein, *Method of Forming Small Geometry Patterns On Piezoelectric Membrane Films*, United States Patent Number 5,403,701, Issued April 4, (1995).

[16] D.H. Turnbull, P.K.Lum, A.T. Kerr, and F.S. Foster, *Simulation of B-Scan Images From Two-Dimensional Transducer Arrays: Part 1 - Methods and Quantitative Contrast Measurements*, Ultrasonic Imaging, Vol 14, 323-343, (1992).

[17] G.R. Harris, Dissertation, *"Transient Ultrasonic Fields - A theoretical Analysis and Experimental Study Using Polyvinylidene Fluoride Piezoelectric Polymer"* (1982).

[18] *E-Fab Stencils* by AMTX, Inc., 5450 Campus Drive, Canandaigua, New York, 14425.

[19] G.M. Sessler, *Piezoelectricity In Polyvinylidenefluoride*, J. Acoust. Soc. Am., 70(6), 1596-1608, (1981).

[20] Solvay Technologies, Inc., 500 Fifth Avenue Suite 3000, New York, New York, 10110.

[21] Dow Corning Corp., Midland, MI 48686.

[22] K. Kimura and H. Ohigashi, *Polarization Behavior Vinylidene Fluoride-Trifluoroethylene Copolymer Thin Films*, Jap. J. of Appl. Phys., Vol 25, No. 3, 383-387, (1986).

[23] K. Koga and H. Ohigashi, Piezoelectricity and Related Properties of Vinylidene Fluoride and Trifluoroethylene Copolymer, Jap. J. of Appl. Phys., Vol 59, No. 6, 2142-2150, (Mar 1986).

[24] Analog Devices, One Technology Way, P.O. Box 9106, Norwood, Mass.,02062-9106, USA.

[25] D.R. Bacon, *Primary Calibration Of Ultrasonic Hydrophones Using Optical Interferometry*, IEEE Trans Ultrasonics, Ferroelectrics, and Frequency Control, Vol 35, No 2, 152-161, (Mar 1988).

[26] D. R. Bacon, *Characteristics Of A PVDF Membrane Hydrophone For Use In The Range 1-100MHz*, IEEE Trans Sonics Ultrason., Vol SU-29, 18-25, (Jan 1982).

[27] D. T. Blackstock, *Connection Between The Fay And Fubini Solutions For Plane Sound Waves Of Finite Amplitude*, The J of the Acoustical Soc of Am, 39,1019-1026, (1966).

[28] T. G. Muir and E. L. Carstensen, *Predictions Of Nonlinear Acoustic Effects At Biomedical Frequencies And Intensities*, Ultrasound In Med. & Biol., Vol 6, 345-357, (1980).

[29] Beyer, R. T., *Nonlinear acoustics, in Physical Ultrasonics*, Academic Press, (1969).

[30] CRC *Standard Mathematical Tables.*

[31] D. R. Bacon, *A New Method For Ultrasonic Hydrophone Calibration*, IEEE Ultrasonics Symposium, 700-704, (1982).

[32] K.J. Parker and E.M. Friets, *On The Measurement Of Shock Waves*, IEEE Trans Ultrasonics, Ferroelectrics, and Frequency Control, Vol 34, No 4, 454-460, (July 1987).

[33] B. A. Herman and G. R. Harris, *Calibration Of Miniature Ultrasonic Receivers Using A Planar Scanning Technique*, J. Acoust. Soc. Am., Vol 72, No 5, 1357-1363, (Nov 1982).

[34] D. G. Shombert, S. W. Smith, and G. R. Harris, *Angular Response Of Miniature Ultrasonic Hydrophones*, Med. Phys., Vol 9, No 4, 484-492, (July/Aug 1982).

[35] R C. Chivers and P. A. Lewin, *The Voltage Sensitivity Of Miniature Piezoelectric Plastic Ultrasonic Probes*, Ultrasonics, Vol 20, 279-281, (1982).

[36] R. C. Chivers and P. A. Lewin, *Voltage Sensitivity Of Miniature Ultrasonic Probes*, Ultrasonics, Vol 21, 282-283, (1983).

[37] G. R. Harris, *Sensitivity Considerations For PVDF Hydrophones Using The Spot-Poled Membrane Design*, IEEE Trans Sonics and Ultrasonics, Vol SU-29, No 6, 370-377, (Nov 1982).

[38] A. S. DeReggi, S. C. Roth, J.M. Kenney, and S. Edelman, G.R. Harris, *Piezoelectric Polymer Probes For Ultrasonic Applications*, J. Acoust. Soc. Am., Vol 69, No 3, 853-859, (Mar 1981).

[39] G. R. Harris, *Hydrophone Measurement In Diagnostic Ultrasound Fields*, IEEE Trans. Ultrasonics, Ferroelectrics, and Frequency Control, Vol 35, No 2, 87-101, (Mar 1988).

[40] P. A. Lewin, M. E. Schafer, and R.C. Chivers, *Integrated Preamplifiers For Ultrasound Transducers*, IEEE Ultrasonics Symposium, 503-506, (1985).

[41] P. Lum, M. Greenstein, C. Grossman Jr, *A High Frequency Hydrophone Developed For Ultrasonic Transducer Field Measurement*, J Ultrasound In Medicine, Vol 14, No 3 (Supplement), S35, (Mar 1995).

[42] G. Ludwig and K. Brendel, *Calibration of Hydrophones Base On Reciprocity and Time Delay Spectrometry*, IEEE Trans Ultrasonics, Ferroelectrics, and Frequency Control, Vol 35, No 2, 168-174, (Mar 1988).

VIII. Figure Captions

Figure 1: Required effective diameter vs. source transducer frequency.

Figure 2: a) The sensitivity for 500 μm diameter hydrophones of various thickness without a cable. b) The sensitivity for 500 μm diameter, 4 μm thick hydrophone with cables of various lengths.

Figure 3: a) Structure for the 3D electrostatic modelling. b) Contours of constant potential at x=50 μm.

Figure 4: a) Photograph of the rear side of the hydrophone, showing the active spot electrode, the ground plane and the on membrane electronics. b) Photomicrograph of the active spot electrode, showing the 37 μm geometric diameter.

Figure 5: a) Waveform of a shock wave from a 20 MHz source transducer, as received by the hydrophone. b) Spectrum of the shock wave showing harmonics up to 315 MHz.

Figure 6: Bandwidth comparison of a) waveform and spectrum for the Marconi hydrophone. b) waveform and spectrum for the present 4 μm hydrophone.

Figure 7: a) Dotted line shows the simulation of a 20 MHz beam at the geometric focus of 19 mm, dashed line is a simulation of a beam measured by a 500 μm diameter hydrophone normalized to the data shown by (x). b) normalized simulation for a hydrophone with a 37 μm diameter.

Figure 8: Plot of the directional response for the present hydrophone.

IX. Table Captions

Table 1: Loaded end-of-cable sensitivity comparison.

Table 1:

		M_L Re 1V/MPa (dB)			
Hydrophone	Amplifier Gain (dB)	5 MHz	10 MHz	15 MHz	20MHz
Marconi	+6	-23.4	-22.2	-20.0	-18.6
Present	+32	-25.1	-23.3	-21.1	-23.6
Difference	+26	-1.7	-1.1	-1.1	-5.0

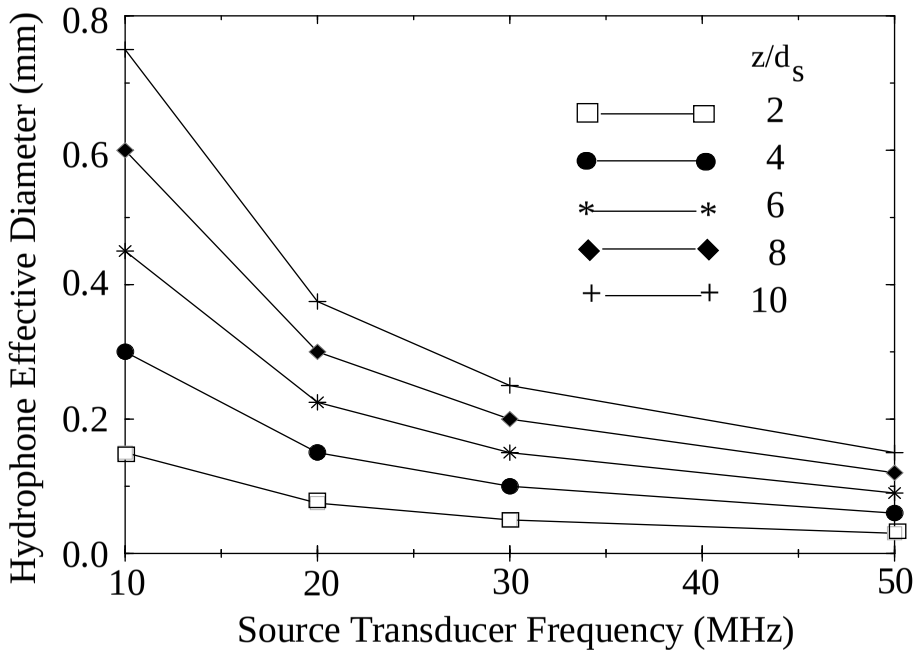

"High Frequency Hydrophone", by Lum etal.

FIG. 1

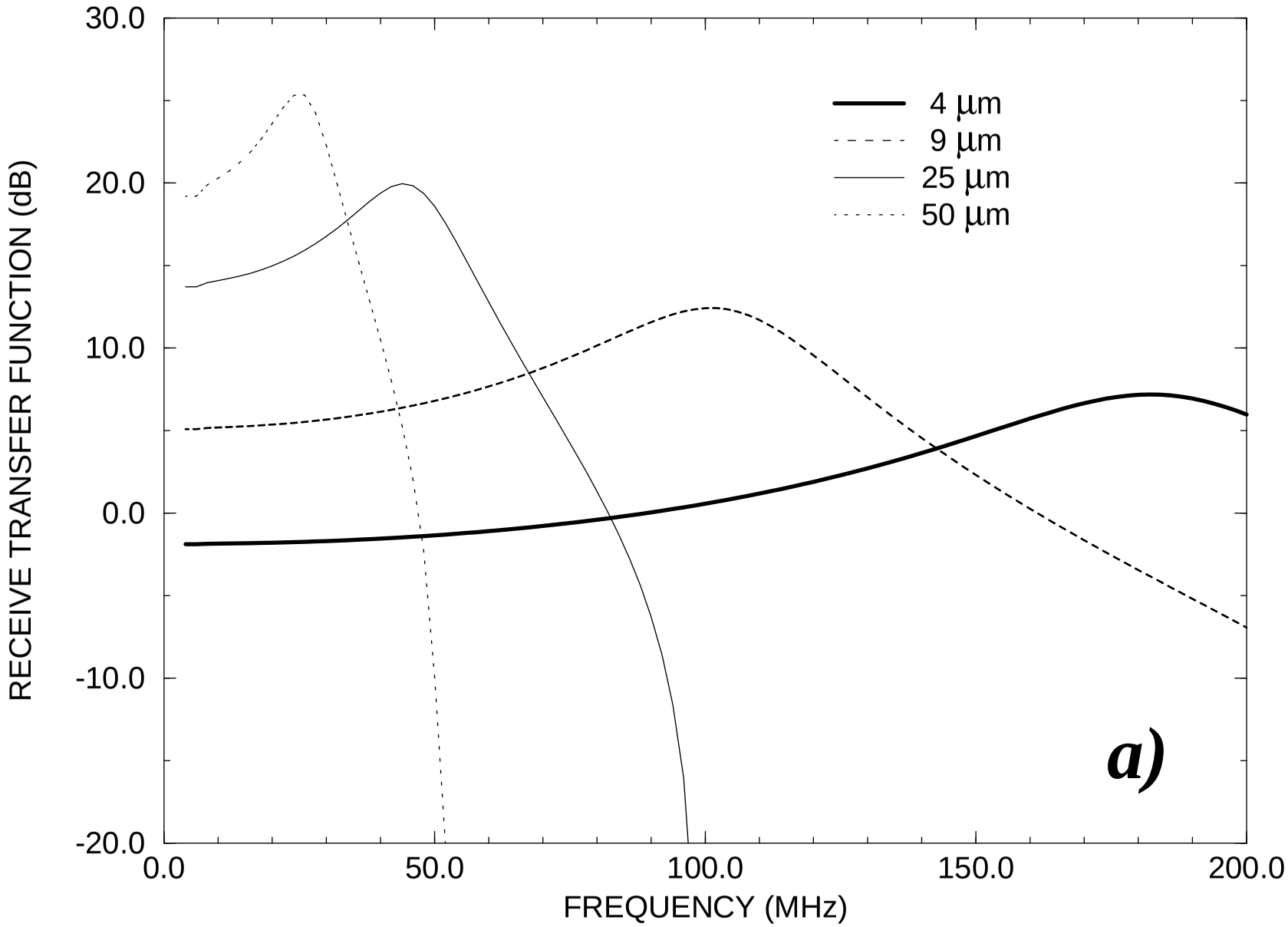

"High Frequency Hydrophone", by Lum etal.

FIG. 2a

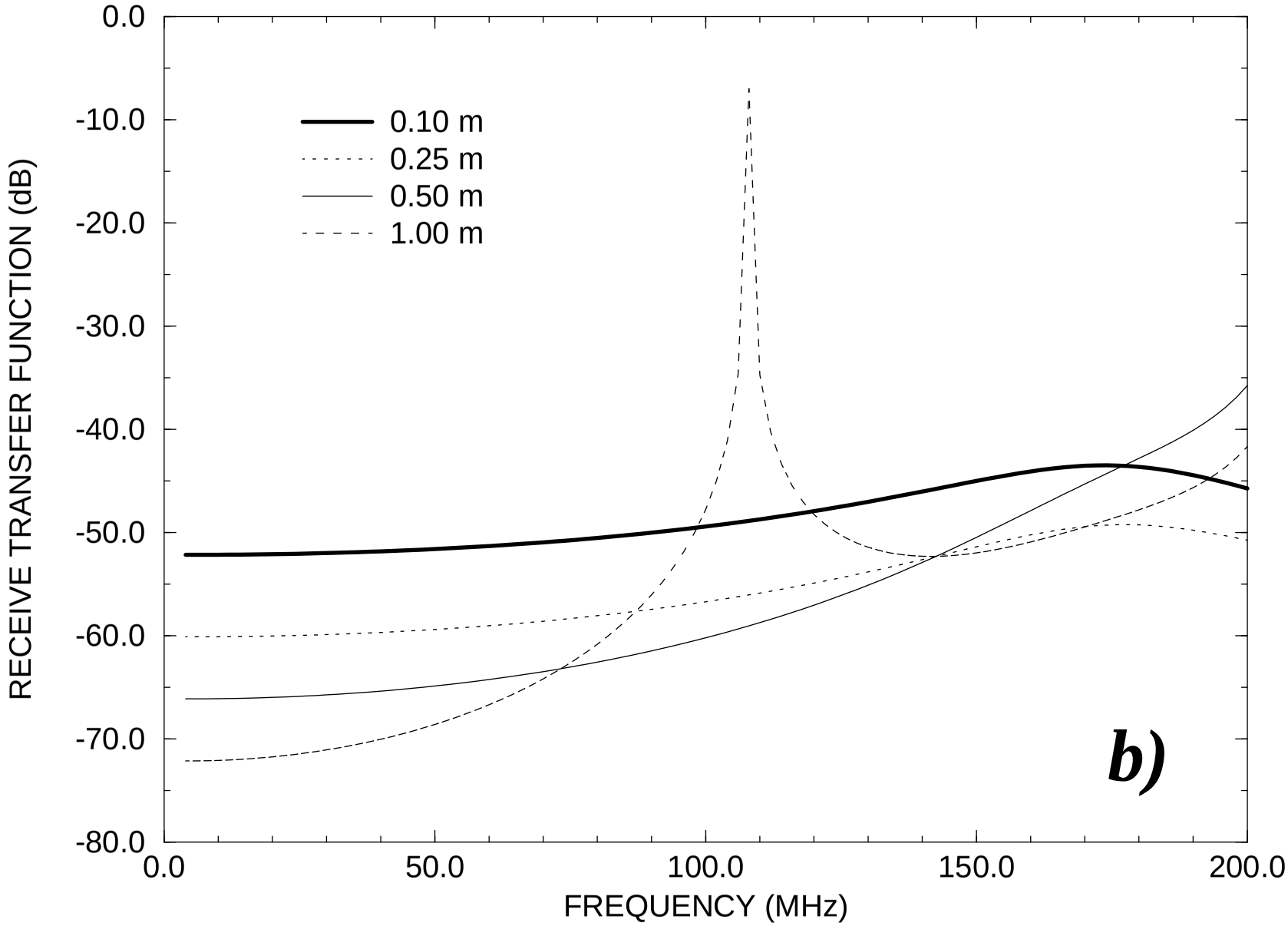

"High Frequency Hydrophone", by Lum etal.

FIG. 2b

3D Structure

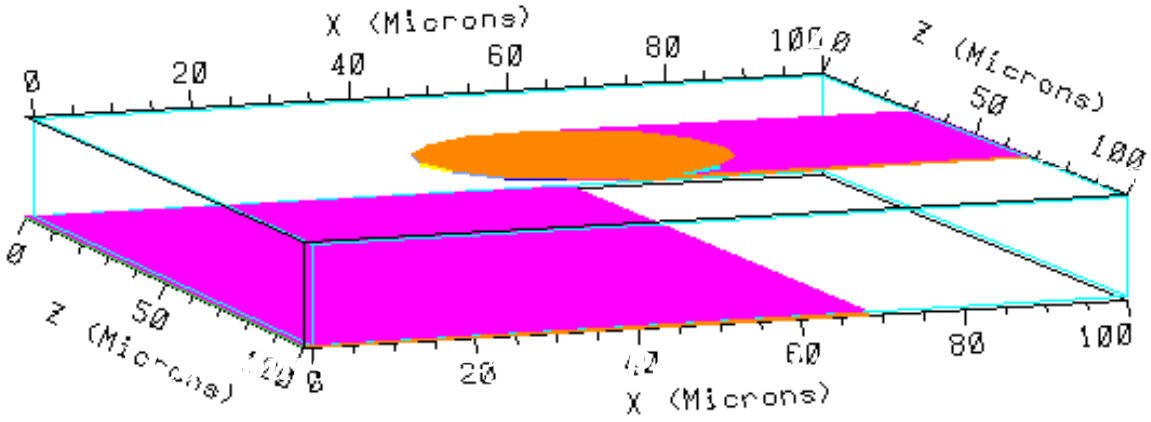

a)

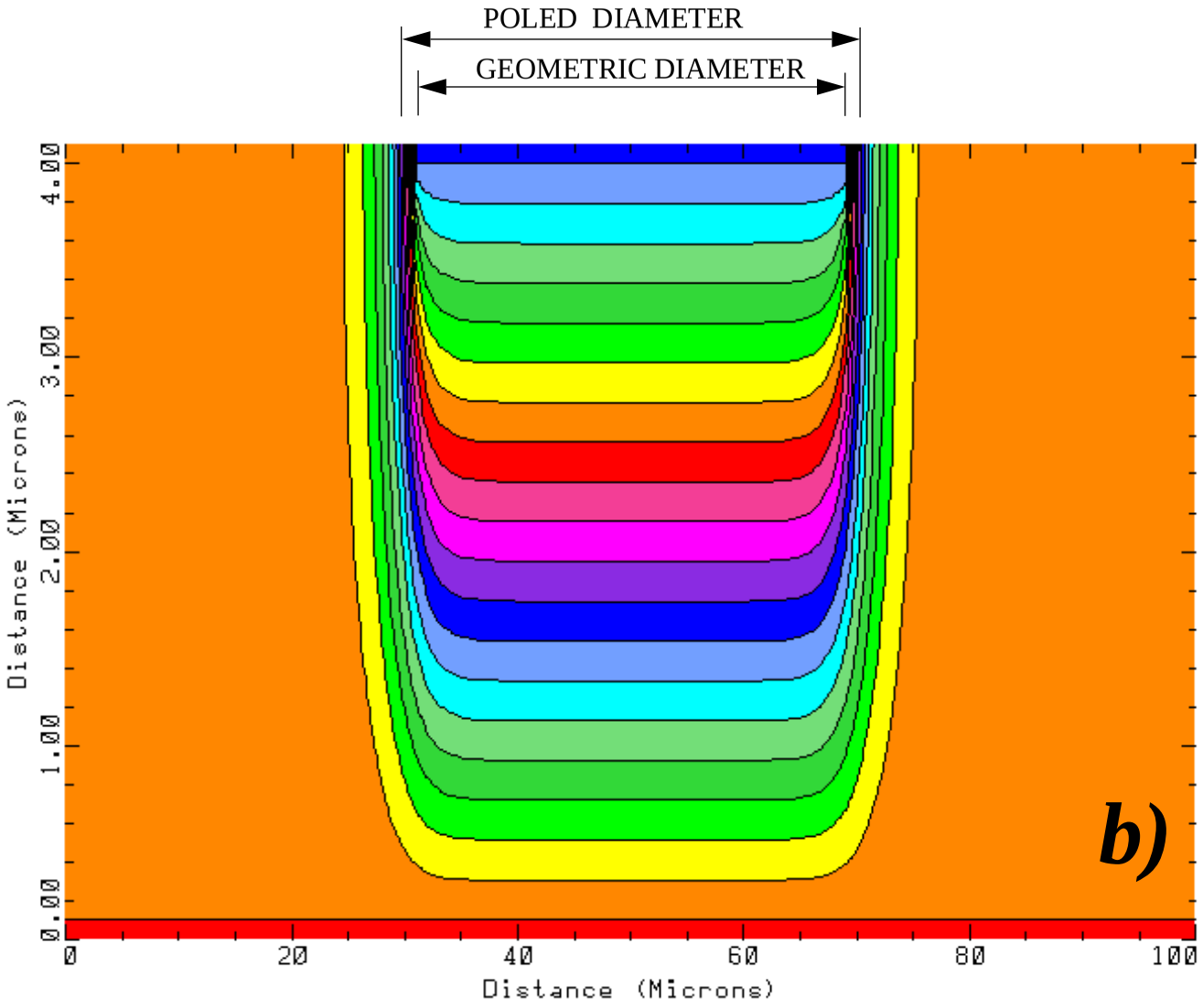

"High Frequency Hydrophone", by Lum etal.

FIG. 3b

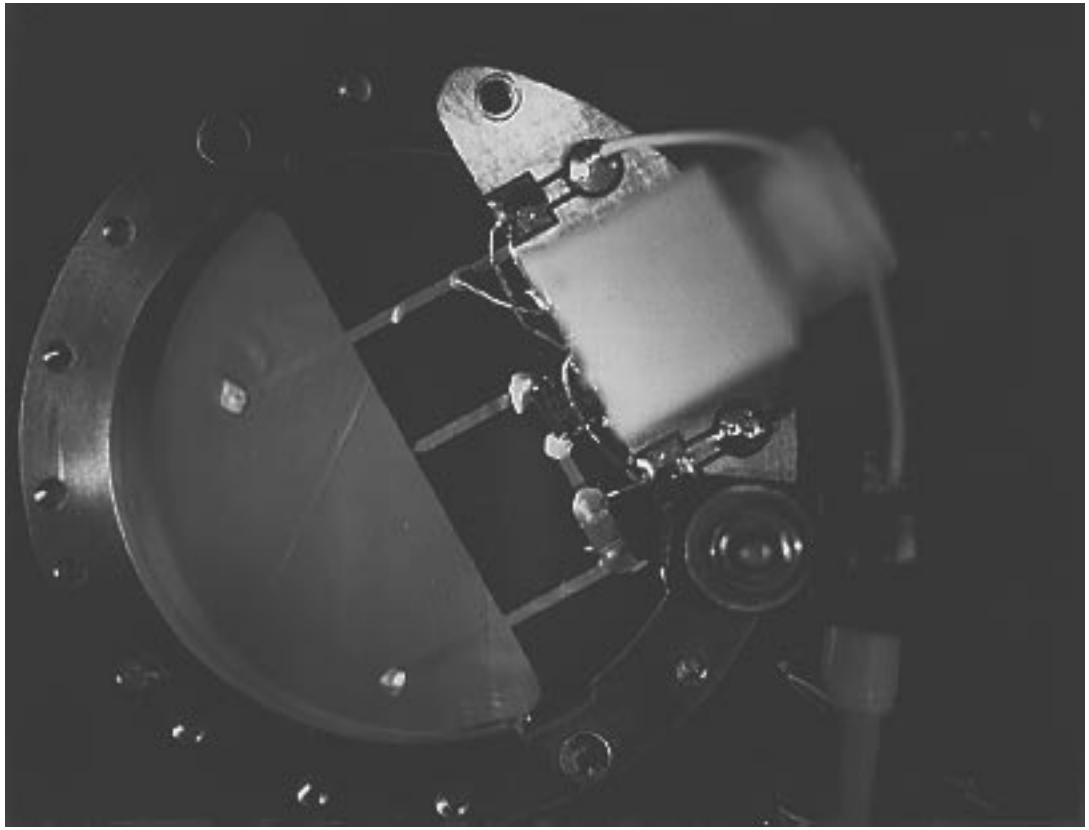

"High Frequency Hydrophone", by Lum etal.

FIG. 4a

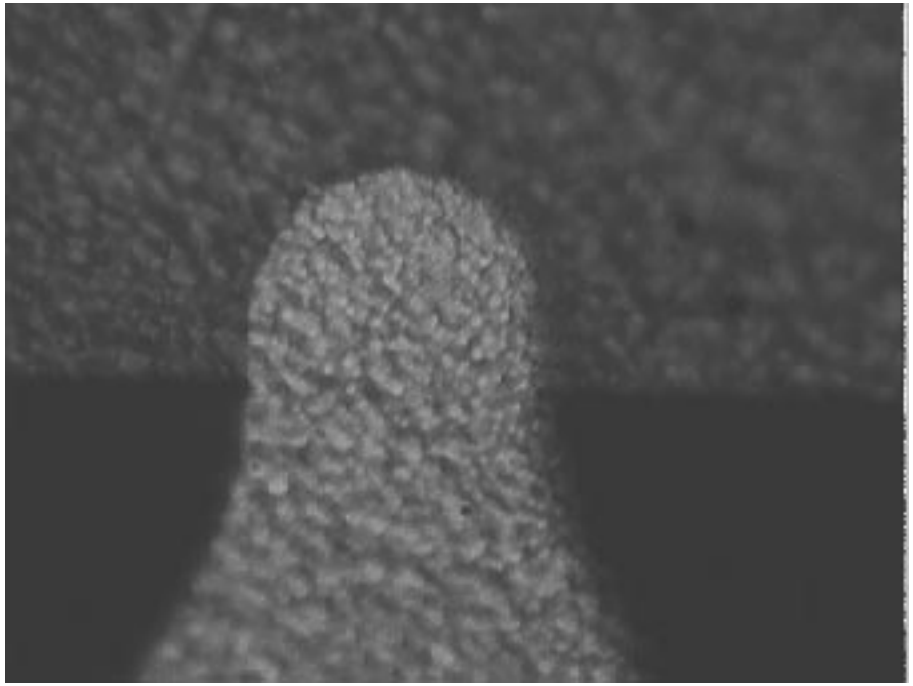

"High Frequency Hydrophone", by Lum etal.

FIG. 4b

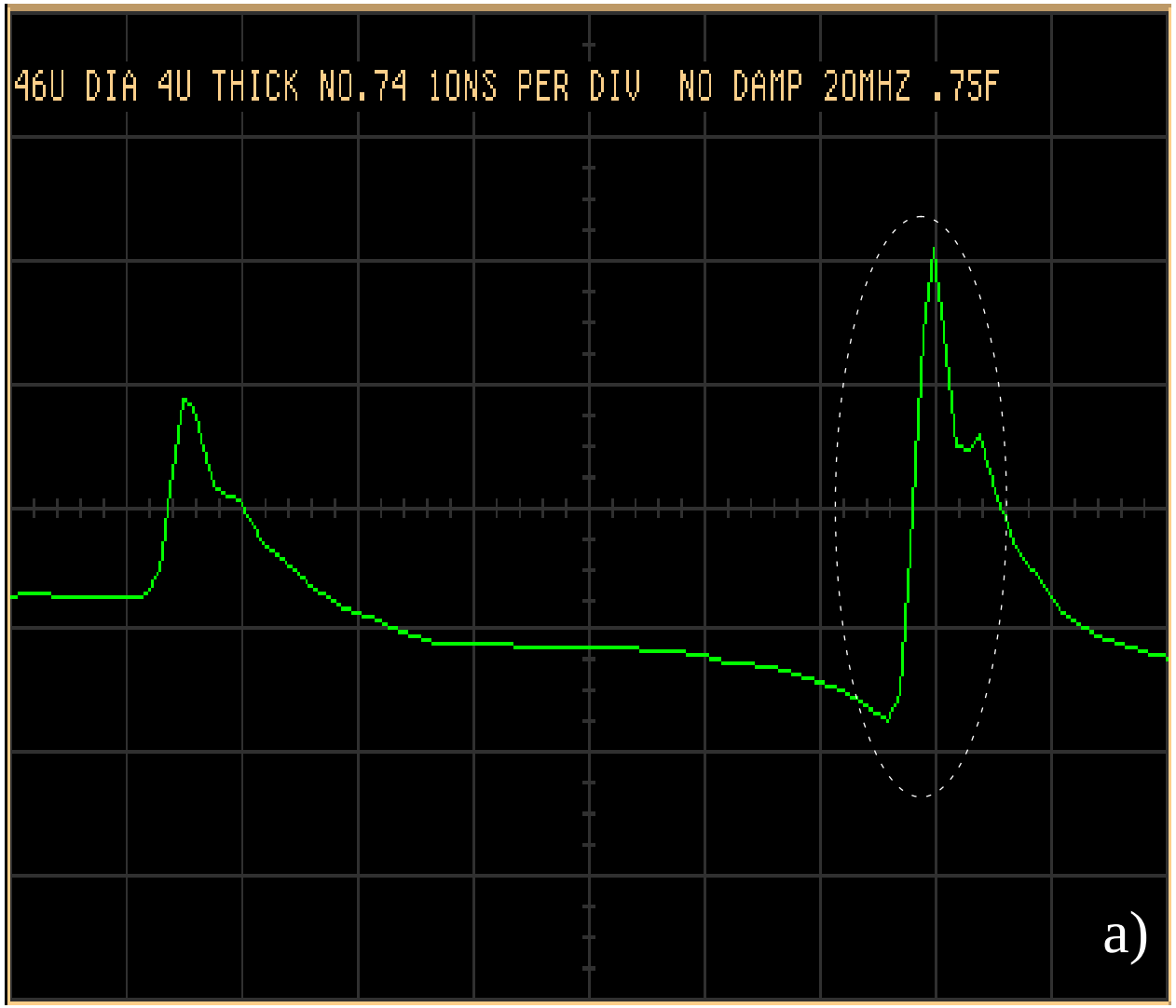
46U DIA 4U THICK NO.74 10NS PER DIV NO DAMP 20MHZ .75F
a)

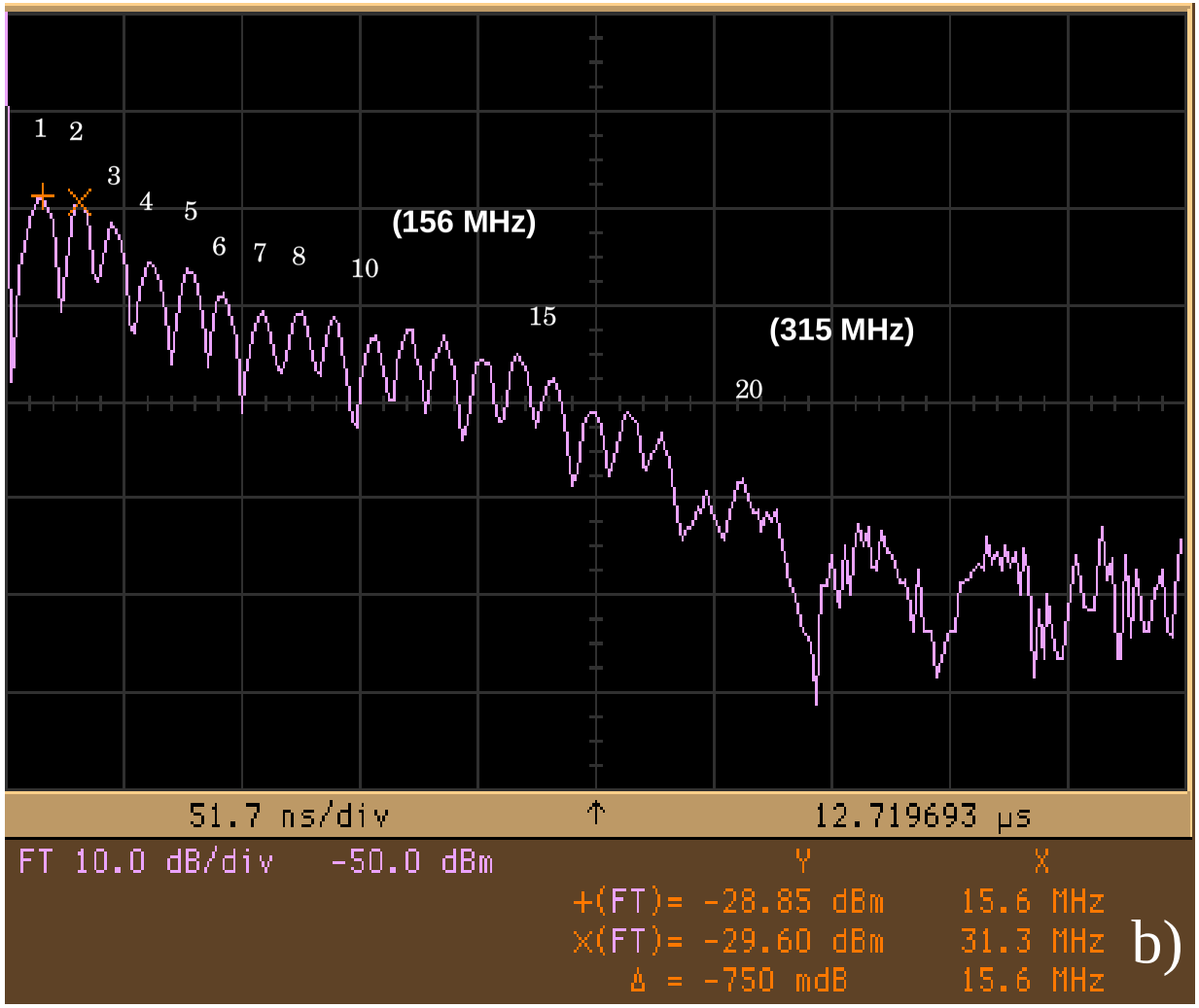
1 2
3
4
5
6
7
8
10
15
20
(156 MHz)
(315 MHz)
51.7 ns/div
12.719693 µs
FT 10.0 dB/div -50.0 dBm
Y X
+(FT)= -28.85 dBm 15.6 MHz
X(FT)= -29.60 dBm 31.3 MHz
Δ = -750 mdB 15.6 MHz
b)

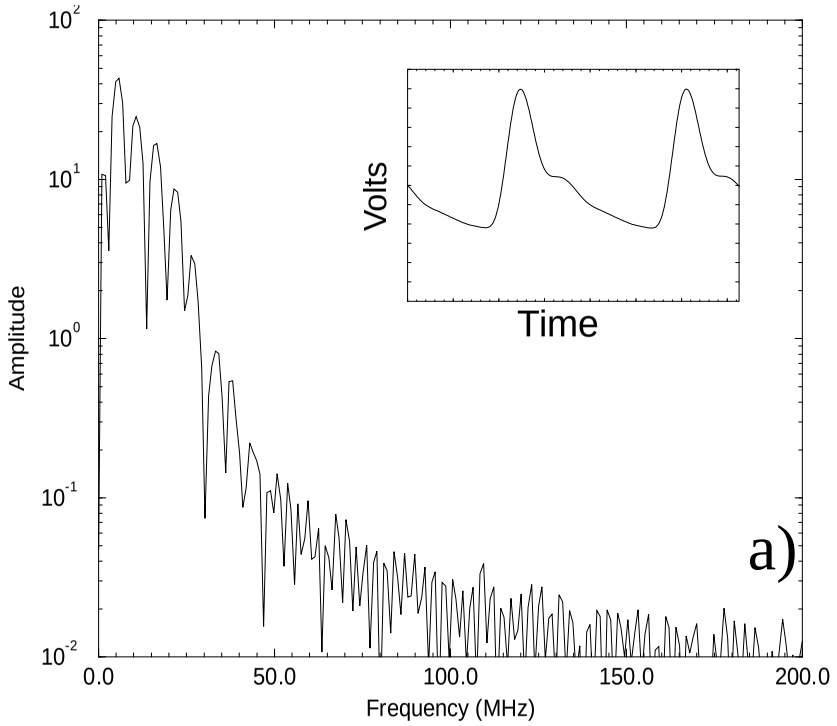

"High Frequency Hydrophone", by Lum etal.

FIG. 6a

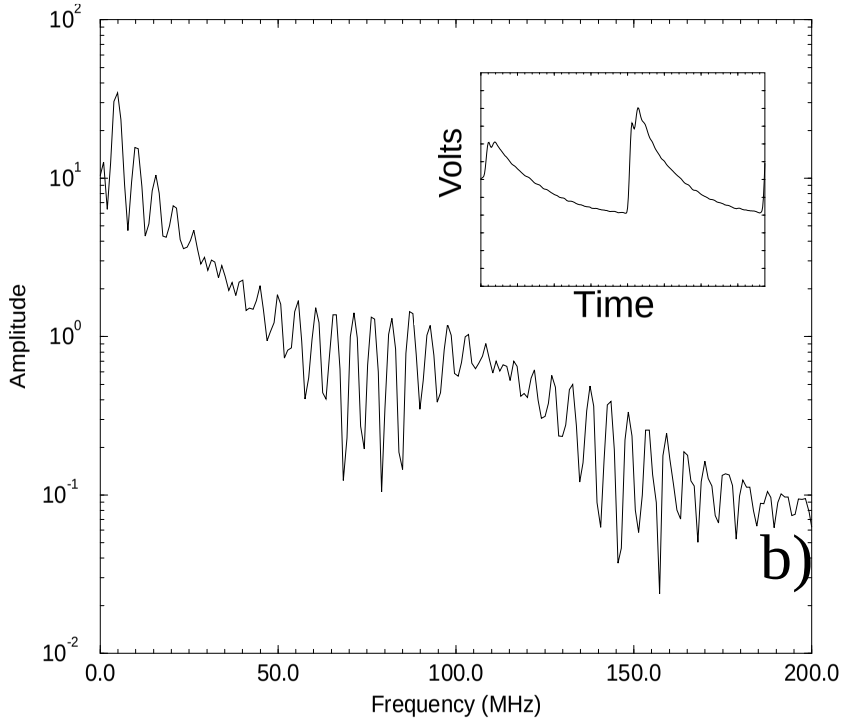

"High Frequency Hydrophone", by Lum etal.

FIG. 6b

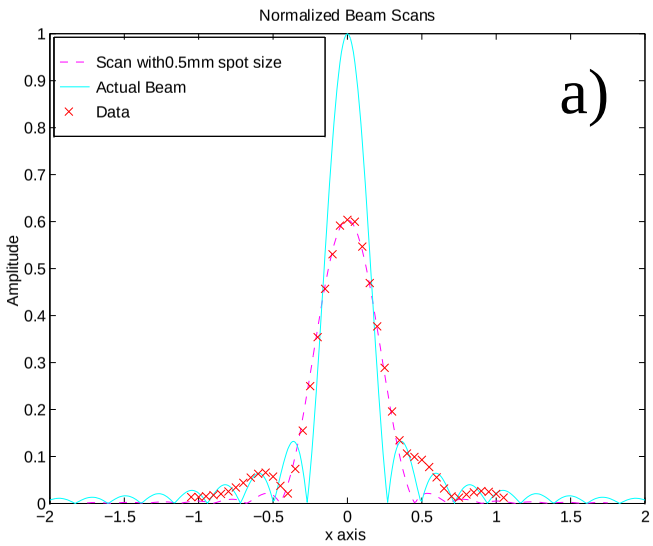
Normalized Beam Scans
Scan with0.5mm spot size
Actual Beam
Data
a)
Amplitude
x axis
0
0.1
0.2
0.3
0.4
0.5
0.6
0.7
0.8
0.9
1
−2
−1.5
−1
−0.5
0
0.5
1
1.5
2

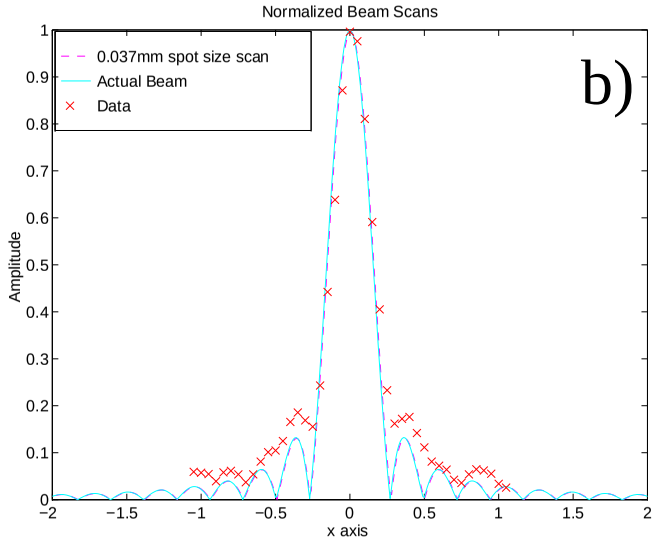
Normalized Beam Scans
0.037mm spot size scan
Actual Beam
Data
b)
Amplitude
x axis
0
0.1
0.2
0.3
0.4
0.5
0.6
0.7
0.8
0.9
1
−2
−1.5
−1
−0.5
0
0.5
1
1.5
2

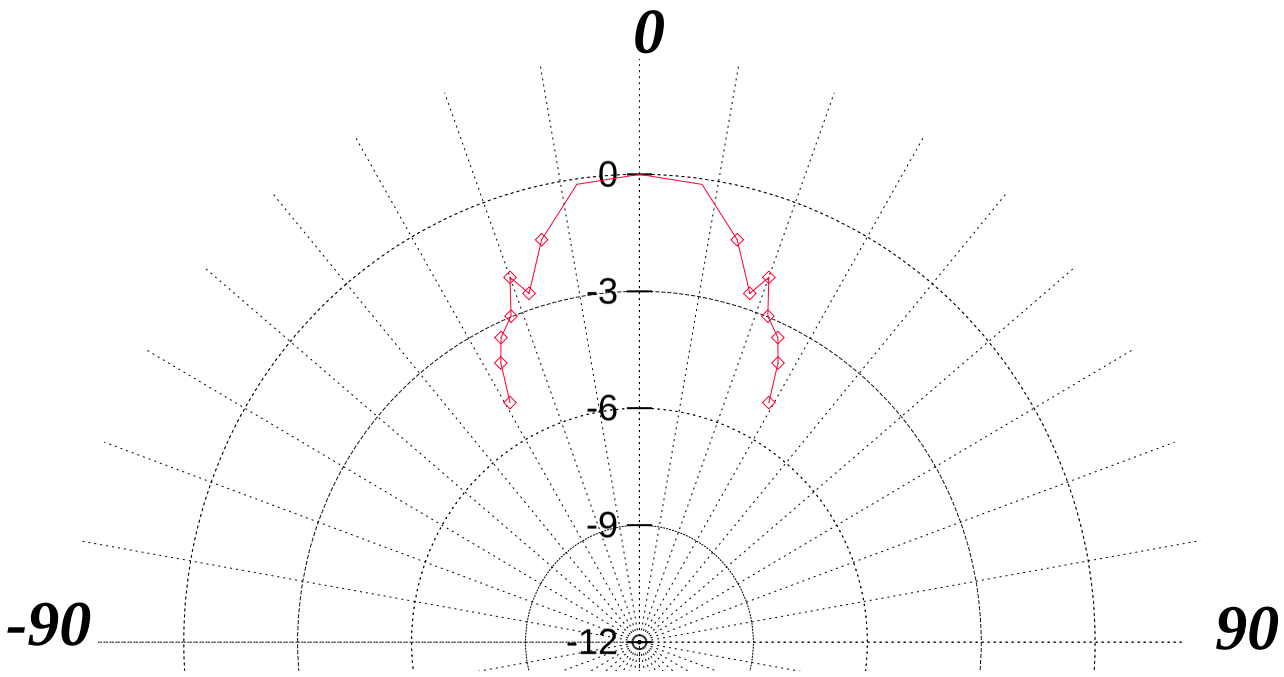

Directional Response (dB)